Contents lists available at ScienceDirect

Results in Physics

results in
PHYSICS

Electrical and thermoelectric properties of nanocrystalline Mn-substituted lithium ferrites

CrossMark

R.P. Patil [a,b,*], B.V. Jadhav [c], P.P. Hankare [a,*]

[a] Department of Chemistry, Shivaji University, Kolhapur 416004, MH, India
[b] Department of Chemistry, M.H. Shinde Mahavidyalaya, Tisangi 416206, MH, India
[c] Department of Chemistry, CKT College Panvel, Mumbai, India

ARTICLE INFO

ABSTRACT

Nanocrystalline Mn-substituted lithium ferrites were synthesized by sol–gel method. The structural data show that, the cubic phase was converted into tetragonal phase observed by XRD analysis. X-ray photoelectron spectroscopy has been used to characterize valence state of materials and the composition of the products. The electrical property study was carried out by using two probe methods and it is revealed that the all Mn substituted ferrites are semiconducting in nature. Thermoelectric power measurement also confirms $1.5 \leqslant x \geqslant 0.0$ N-type and $2.5 \leqslant x \geqslant 2.0$ shows the P-type semiconducting nature of Mn-substituted lithium ferrites. The effect of manganese substitution in lithium ferrites has a crucial role on the structural and electrical properties of the system.

1. Introduction

Lithium ferrites have been studied and developed for many years because of their electrical, magnetic and structural properties that provide applications of scientific and technological interest [1–3], determined by their chemical composition and microstructure [4,5]. Many transition metal cations such as Mn, Cr, Co and Ti can be introduced into the lattice of the magnetic structure, which is related to a large number of applications [6–9]. Three types of ferrites can be considered: spinel, garnet and hexaferrite [10]. In the spinel structure of general formula AB_2O_4 there are twice as many octahedral (B) sites as tetrahedral (A) sites. If M^{2+} occupies only the A sites, the spinel is normal; if it occupies only the B sites, the spinel is inverse. Mixed-metal oxides have a very important role in the field of electronic devices, as fluids, catalytic activity and sensors due to the very important structural and electrical properties. Lithium ferrites in the spinel phase, $Li_{0.5}Fe_{2.5}O_4$, have a square hysteresis loop, high magnetization and high Curie temperature. These properties are useful for technological applications such as the development of low-cost material microwave devices. Various methods have been developed for the synthesis

of ferrites [11–15] but, in this study, the sol–gel autocombustion is used. Lithium and metal substituted lithium ferrites are more applicable in the field of lithium batteries, therefore we have developed the Mn-substituted lithium ferrite system by using sol–gel method. Sol–gel method is a useful technique when compared to other methods, due to the better homogeneity, smaller particle size and modification of surface area. In the present investigation, we have developed Mn-substituted lithium ferrites by using the sol–gel method and characterized by X-ray diffraction to structural analysis, electrical properties of system also studied by two-probe method. Thermoelectric properties of Mn-substituted lithium ferrites were also carried out. The electrical and structural properties of Mn-substituted lithium ferrites were characterized by using X-ray diffraction (XRD), X-ray photoelectron spectroscopy (XPS) and electrical study by using two probe electrical circuits.

2. Experimental techniques

Polycrystalline ferrite samples having the general formula, $Li_{0.5-}Fe_{2.5-x}Mn_xO_4$ ($x = 0.0, 0.5, 1.0, 1.5, 2.0$ and 2.5) were synthesized by the sol–gel method and flow diagram for the synthesis technique is shown in Fig. 1. High purity AR grade ferric nitrate, manganese nitrate, lithium nitrate and citric acid were used for synthesis. The metal nitrate solutions were mixed in the required stoichiometric ratios in distilled water. The pH of the solution was maintained between 9 and 9.5 by using ammonia solution. The solution mixture was slowly heated to 373 K with constant stirring to obtain a fluppy mass. The precursor powder was sintered at 973 K for 8 h. The

* Corresponding authors. Tel.: +91 231 2609381.
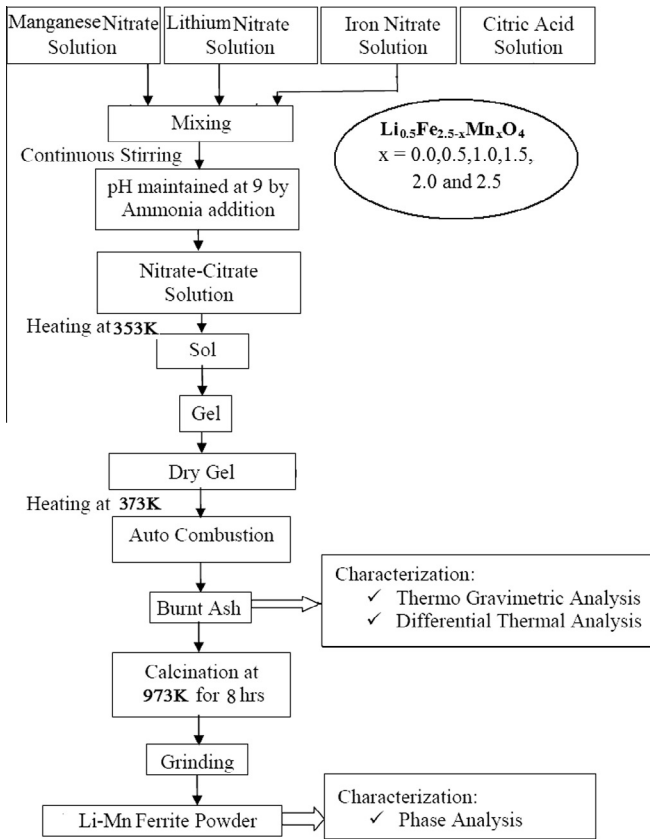E-mail addresses: raj_rbm_raj@yahoo.co.in (R.P. Patil), p_hankarep@rediffmail.com (P.P. Hankare).

Fig. 1. Flow diagram for sol–gel technique.

sintered powder was mixed with 2% polyvinyl alcohol as a binder and uniaxially pressed at a pressure of 8 tons/cm^2 to form pellets.

2.1. Characterizations

The phase formation of the samples was confirmed by X-ray diffraction studies using a Philips PW-1710 X-ray diffractometer with CuKα radiation (λ = 1.54056 Å). The SEM micrograph of the samples was obtained using scanning electron microscope (JEOL JSM 6360). The XPS study was carried out by Phi560 XPS/AES/SIMS UHV system. Electrical properties of all the samples were studied by using two-probe method.

3. Results and discussion

3.1. Phase formation

3.1.1. Thermogravimetric analysis

TG and DTA curves for the dried sample of Li$_{0.5}$Fe$_{1.5}$Mn$_{1.0}$O$_4$ sample are presented in Fig. 2. As shown in the figure, in the TG curve, the percent weight loss with the temperature is observed. A continuous weight loss was observed from TG curve up to 600 °C of the sample in the formation of a stable oxide compound. However DTA curves show one exothermic peak around 290 °C. At this temperature, a decomposition of mixed-metal citrate complexes by fragmentation and thermal degradation of organic content occurs and this results in the formation of stable mixed-metal oxides.

3.1.2. XRD studies

X-ray diffraction patterns of the Mn-substituted lithium ferrite samples are shown in Fig. 3. A definite line broadening of the diffraction peaks indicated that, the prepared ferrospinels are in the nanometer range. From the X-ray diffraction peaks, average particle size was estimated using Scherrer's formula.

$$t = 0.9\lambda/\beta\cos\theta$$

where, symbols have usual meaning.

The manganese substituted lithium ferrite systems, Li$_{0.5}$Fe$_{2.5-x}$Mn$_x$O$_4$ are seen to be cubic in the range $1.5 \leqslant x \geqslant 0.0$ and tetragonal spinel phase in the range of $2.5 \leqslant x \geqslant 2.0$. The tetragonal structure for $x = 2.0$ and 2.5 is due to the Jahn–Teller effect by Mn^{3+} ions with d^4 electron configuration [16–18] and more than 50% manganese ions at the B sites to cause tetragonal distortion in the lattice. The lattice constant increases with substitution of manganese content up to $x = 1.5$, there after decreases due to the tetragonal distortion. The increase in the lattice constant with an
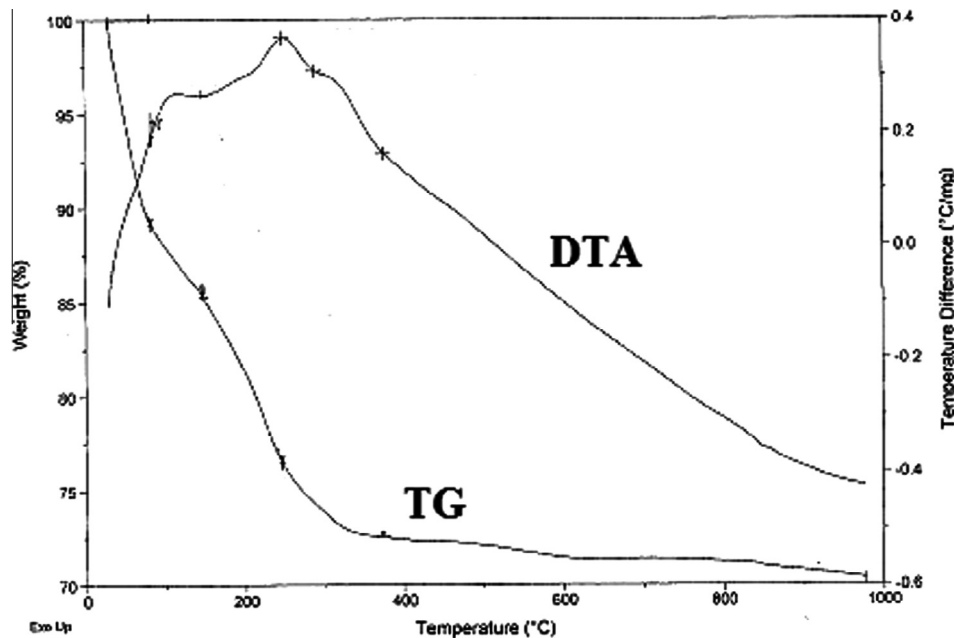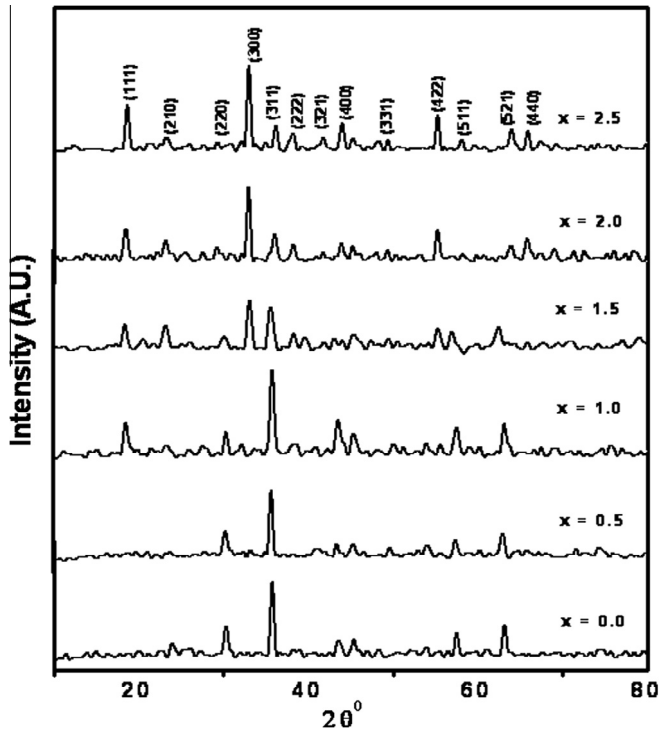

Fig. 2. TGA-DTA Spectrum for Li$_{0.5}$Fe$_{1.5}$Mn$_{1.0}$O$_4$.

Fig. 3. X-ray diffraction patterns of $Li_{0.5}Fe_{2.5-x}Mn_xO_4$ system.

Table 1
Lattice constant, crystallite size and x-ray density for $Li_{0.5}Fe_{2.5-x}Mn_xO_4$ system.

Composition (x)	Lattice constant (a) Å	Crystallite size (t) nm	X-ray density (dx) gm/cm³
0.0	8.30	29	4.8
0.5	8.32	32	4.7
1.0	8.33	32	4.7
1.5	8.39	32	4.6
2.0	$a = b = 5.6724$, $c = 8.747$	33	4.9
2.5	$a = b = 5.4194$, $c = 9.666$	33	5.0

increase in Mn is due to the higher ionic radii of Mn^{3+} (0.645 Å) ions as compared to Fe^{3+} (0.64 Å) ions as shown in Table 1. The X-ray density (dx) was calculated using the following relation.

$$dx = 8M/Na^3$$

where, N = Avagodro's number (6.023 × 10²³ atom/mole), M = Molecular weight, a = Lattice constant.

The values of lattice constant (a), x-ray density (dx), crystallite size and Curie temperature are summarized in Table 1.

3.2. Scanning electron microscopy

The SEM images of Mn-substituted lithium ferrites are shown in the Fig. 4. It is observed that, the average grain size goes on increasing on substitution of Mn content. The average grain size was smaller than 0.1 μm for all the compositions.

3.3. X-ray photoelectron spectroscopy

X-ray photoelectron spectroscopy (XPS) has been widely used to characterize the valence state of materials. Binding energies (BE) are used to identify different elements and their valence
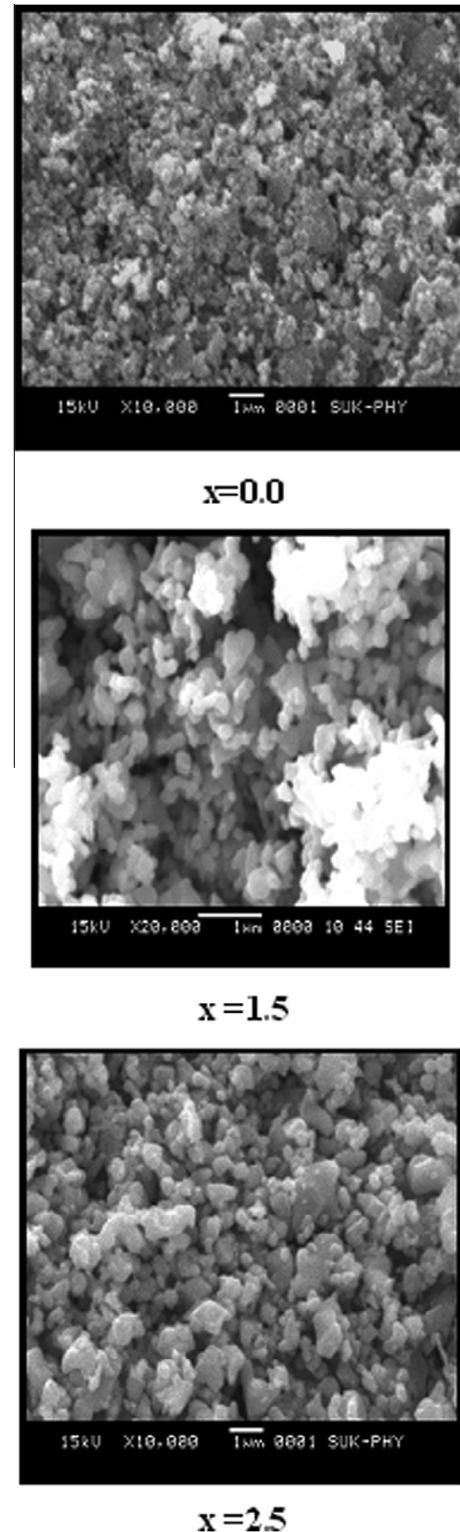

x=0.0

x=1.5

x=2.5

Fig. 4. SEM images of $Li_{0.5}Fe_{2.5-x}Mn_xO_4$ system x = 0.0, 1.5 and 2.5.

states. Moreover, using the relative area under the deconvoluted XPS bands, we can obtain a semiquantitative estimation of the valence states of the elements in the mixed-valent compounds. Fig. 5 presents the typical full-scale XPS spectra of $Li_{0.5}Mn_{1.5}Fe_{1.0}O_4$. The figures show that the binding energies relating to Li 1s, Fe $2p_{3/2}$, and Fe $2p_{1/2}$ are about 55.8, 710.8, and 724.7 eV, respectively. The data are consistent with the values reported for lithium ferrite
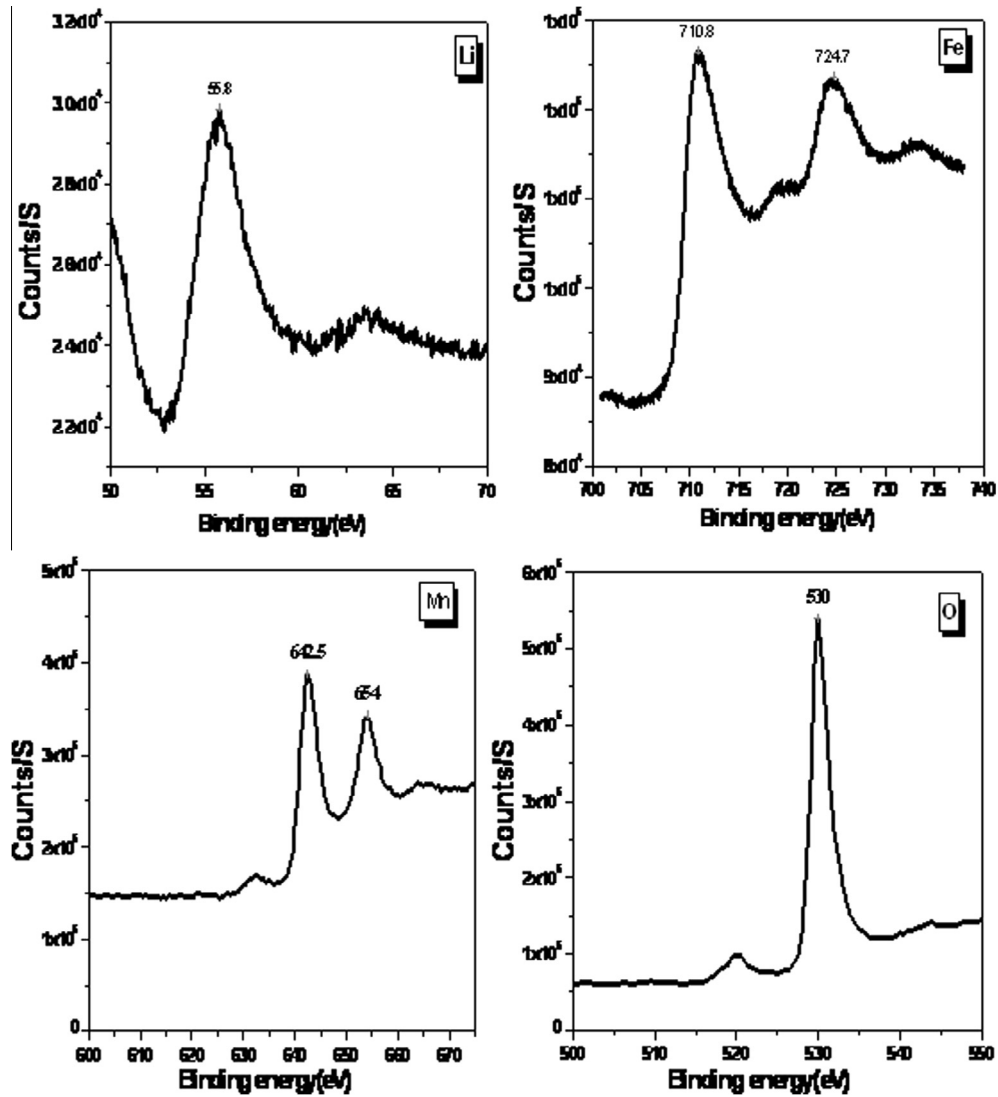
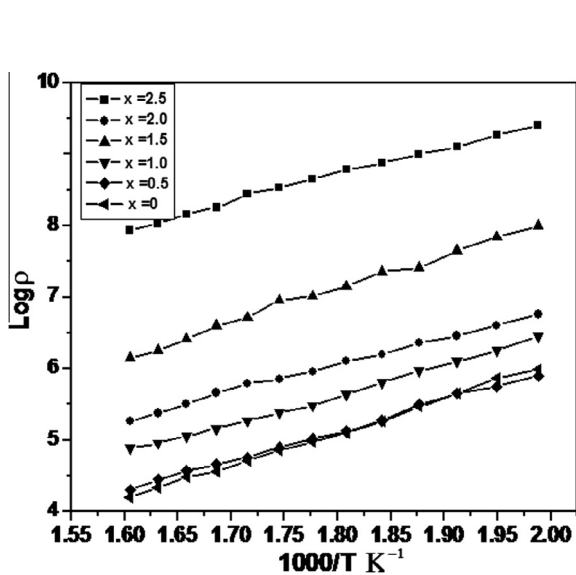**Fig. 5.** XPS spectra for Li$_{0.5}$Mn$_{1.5}$Fe$_{1.0}$O$_4$ sample.

Fig. 6. Electrical conductivity study of Li$_{0.5}$Fe$_{2.5-x}$Mn$_x$O$_4$ system.

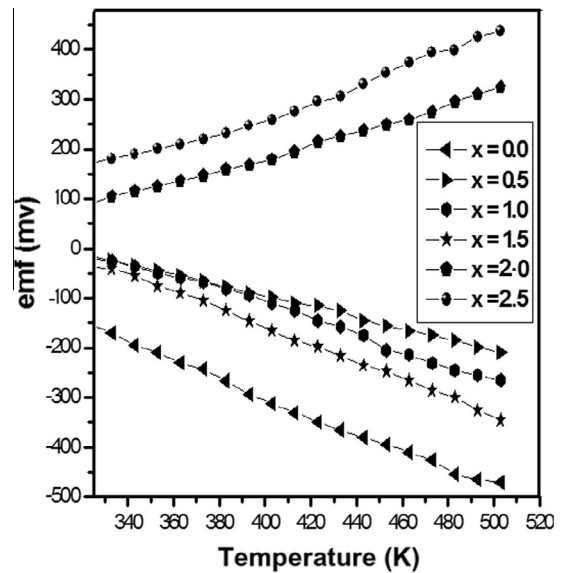**Fig. 7.** Thermoelectric power measurement study of Li$_{0.5}$Fe$_{2.5-x}$Mn$_x$O$_4$ system.

in the literature [19]. Therefore, XPS results also prove the composition of the products. The Fe 2p spectra recorded from one sample are characterized by binding energies of the Fe $2p_{3/2}$ and Fe $2p_{1/2}$ core levels of 710.2 and 723.9 eV, respectively, which is indicative of the presence of Fe^{3+}. The low-energy band located at about 54 eV is assigned to Li 1s. The band at about 530 eV is assigned to O 1s. Mn $2p_{3/2}$ and Mn $2p_{1/2}$ are responsible for the bands at about 642.5 and 654 eV, respectively. Chowdari has reported that the Mn $2p_{3/2}$ XPS binding energy of Mn^{3+} and Mn^{4+} ions is at 641.9 and 643.2 eV, respectively. In our experiment, the Mn $2p_{3/2}$ binding energy of the samples is in this region, which indicates that the Mn valence in $Li_{0.5}Mn_{1.5}Fe_{1.0}O_4$ is in the mixed valence state. The relative amounts of Mn^{3+} and Mn^{4+} ions in $Li_{0.5}Mn_{1.5}Fe_{1.0}O_4$ can be estimated by deconvoluting the asymmetric Mn $2p_{3/2}$. XPS spectra, using the dominant Mn^{3+} and Mn^{4+} BE values of 641.5 and 654 eV, respectively, as shown in Fig. 5.

3.4. Electrical study

Electrical resistivity (ρ) of samples was studied over the temperature range from room temperature to 623 K and is shown in Fig. 6. It can be seen that the resistivity decreases with increasing temperature for all samples. The observed behavior clearly indicates that the present Mn-substituted lithium ferrites have semiconductor like behavior. The change in electrical resistivity is due to the presence of Fe^{2+} ions. The decrease in resistivity due to the mobility of the extra electron, comes from Fe^{2+} through the crystal lattice. The figure shows the plots of log ρ vs. 1000/T for all the samples which are almost linear without any break indicating their semiconducting nature. The relationship $\rho = \rho_o \exp \Delta E/KT$ (where, ρ = resistivity in ohm cm, ρ_o = constant or weak function of temperature, ΔE = energy of activation, K = Boltzmann constant, T = absolute temperature in K) is found to be obeyed for all compositions. A detailed study of electrical resistivity shows that as Mn ion concentration increases electrical resistivity increases. The maximum resistivity was observed for $Li_{0.5}Mn_{2.5}O_4$ sample.

3.5. Thermoelectric power measurement

The composition variation of see back coefficient as a function temperature is shown in Fig. 7. The samples x = 0, 0.5, 1.0 and 1.5 show N-type and x = 2.0 and 2.5 show P-type conductivity. The conduction mechanism in N-type specimens is predominantly due to the electrons from Fe^{2+} to Fe^{3+} ions, whereas in the p type it is due to hole transfer from Mn^{3+} to Mn^{4+} ions. The appearance of 'p' type carriers in the present case is due to the hole transfer in Mn^{3+} to Mn^{4+} while Fe^{2+} to Fe^{3+} gives rise to 'n' type charge carriers.

4. Conclusions

In conclusion, a nanocrystalline Mn substituted lithium ferrite sample has been prepared successfully using the sol–gel method. The structural data show that, the cubic phase was converted into tetragonal phase observed by XRD analysis. XPS study shows that valence state of materials. The DC conductivity is increasing with increasing temperature for all the samples indicating that Mn-added lithium ferrites have semiconductor-like behavior. Thermoelectric power measurement also confirms $1.5 \leqslant x \geqslant 0.0$ N-type and $2.5 \leqslant x \geqslant 2.0$ shows P-type semiconducting nature.

References

[1] Ramachandran N, Biswas ABJ. Solid State Chem 1979;30:61–4.
[2] Shirane T, Kanno R, Kawamoto Y, Takeda Y, Takano M, Kamiyama T, et al. Solid State Ionics 1995;79:227–33.
[3] Tabuchi M et al. J Solid State Chem 1998;141:554–61.
[4] Smit J, Wijn HPJ. Ferrites. NewYork: Wiley; 1959 [p. 158].
[5] Igarashi H, Okazaki K. J Am Ceram Soc 1977;60:51.
[6] Gadkari AB, Shinde TJ, Vasambekar PN. Mater Chem Phys 2008;114:505–10.
[7] Argentina GM, Baba PD. IEEE Trans Microw Theory Tech 1974;22:652–8.
[8] Hankare PP, Patil RP, Sankpal UB, Jadhav SD, Lokhande PD, Jadhav KM, Sasikala R. J Solid State Chem 2009;182:3217.
[9] Hankare PP, Patil RP, Sankpal UB, Jadhav SD, Mulla IS, Jadhav KM, Chougule BK. J Magn Magn Mater 2009;321:3270.
[10] Teo MLS, Kong LB, Li ZW, Lin GQ, Gan YB. J Alloys Compd 2007;459:557.
[11] Huo J, Wei M. Mater Lett 2009;63:1183.
[12] Cook W, Manley M. J Solid State Chem 2010;183:322.
[13] Jiang XN, Lan ZW, Yu Z, Liu PY, Chen DZ, Liu CY. J Magn Magn Mater 2009;321:52.
[14] Berbenni V, Marini A, Matteazzi P, Ricceri R, Welham NJ. J Acknowledge Eur Ceram Soc 2002;23:527.
[15] Figueiro SD, Goes JC, Moreira RA, Sombra ASB. Carbohydr Polym 2004;56:313.
[16] Tarascon JM, Wang E, Shokoohi FK. J Electrochem Soc 1991;138:2859.
[17] M Thackeray M, David WIF, Bruce DG, Goodenough JB. Mater Res Bull 1983;18:461.
[18] Ohzuku T, Kitagawa M, Hirai TJ. Electrochem Soc 1990;137:769.
[19] Ahniyaz A, Fujiwara T, Song SW, Yoshimura M. Solid State Ionics 2002;151:419. http://dx.doi.org/10.1016/S0167-2738(02)00548-9.